

RESEARCH

Open Access



What is the appropriate axial position in cannulated screw fixation for femoral neck fractures? A finite element analysis

Dae-Kyung Kwak^{1†}, Yeji Lee^{2†}, Sung-Jae Lee², Seunghun Lee¹ and Je-Hyun Yoo^{1*}

Abstract

Background Cannulated screw fixation is a common surgical treatment for femoral neck fractures; however, there is limited information on the optimal axial position of the screws. Herein, we aimed to investigate the impact of axial screw position on surgical stability in femoral neck fracture models fixed with three cannulated screws.

Methods Eighteen finite element models (FEMs) replicating Pauwels type II femoral neck fractures were constructed and tested using nine normal and nine osteoporotic bone models. Each FEM simulated combinations of three different screw positions (anterior, central, and posterior) in the axial view and three models (type 1: 8° angles, 10 mm inter-screw interval; type 2: 6° angles, 10 mm inter-screw interval; type 3: 8° angles, 6 mm inter-screw interval), assuming anatomical reduction. Stress concentrations on the screws and bone were investigated, with measurements of peak von Mises stress (PVMS) and mean stress.

Results Stress concentration on the cannulated screws was consistently observed at the inferior screw near the fracture site in all FEMs. Stress concentrations on the bone around the screws were noted around the head and tip of the inferior screw in each FEM. All PVMS on the screw and surrounding bone decreased as the screw position moved from posterior to anterior in the axial view. Additionally, these stresses decreased as the screw tilt angle increased and the inter-screw interval was maximized. The mean stresses over the region of interest in all FEMs showed similar patterns to those of the PVMSs.

Conclusion To enhance fixation stability and reduce stress concentrations at the fracture site and lateral cortex in femoral neck fractures fixed with three cannulated screws, positioning the screws anterior to the center in the axial view and maximizing the inter-screw interval, tailored to the patient's femur geometry, are recommended.

Keywords Femoral neck fractures, Cannulated screws, Axial position

[†]Dae-Kyung Kwak and Yeji Lee contributed equally to this work.

*Correspondence:

Je-Hyun Yoo
oships@hallym.ac.kr

¹Department of Orthopaedic Surgery, Hallym University Sacred Heart Hospital, Hallym University School of Medicine, Anyang, South Korea

²Department of Biomedical Engineering, Inje University, Gimhae, South Korea



Background

Femoral neck fractures are commonly precipitated by osteoporosis in the elderly and by high-energy trauma in young adults [1]. In young patients, femoral neck fractures, and non-displaced fractures in elderly patients, typically require hip-conserving surgeries [2, 3]. The aim of surgical treatment is to achieve union through anatomical reduction and stable fixation without complications. Various devices, such as multiple cannulated screws or dynamic hip screws, are widely used for this purpose [4, 5]. Additionally, recent advancements have introduced various internal fixation techniques such as the Femoral Neck System (Depuy Synthes, Switzerland), additional parallel four-screw fixation, alpha fixation, and buttress plating, all aimed at reducing fixation failure and other complications [6–8]. Despite these advancements, fixation failures still occur (11 to 32%), and the optimal fixation method remains controversial [9–12].

Cannulated screws continue to be favored for their minimal invasiveness, ease of handling, and ability to induce dynamic compression [2]. Several authors advocate for placing the screws in an inverted triangle configuration, as wide as possible, to enhance stability [10, 13]. Even with anatomical reduction and correct screw placement, fixation failure or femoral neck shortening can frequently occur [14].

Femoral neck collapse after cannulated screw fixation can occur not only in the coronal plane but also in the axial plane [15]. Zhang et al. reported that inferior fully threaded screws can decrease varus deformity in the coronal plane and reduce fixation failure after using three cannulated screws [16]. Similarly, Shin et al. suggested that positioning a fully threaded screw posteriorly can prevent posterior neck collapse [15]. A recent biomechanical study reported that posterior neck comminution and posterior tilt of the femoral neck after cannulated screw fixation are frequently encountered problems and the reasons for loss of reduction, further femoral neck collapse, and nonunion [17]. As such, various cannulated screw fixation techniques and positions have been explored to enhance fixation stability in the anteroposterior (AP) view of femoral neck fractures [6, 18, 19]. Nonetheless, information on the optimal axial position of screws for increasing fixation stability during three-screw fixation of femoral neck fractures remains scarce. Therefore, we conducted this finite element analysis (FEA) study to mechanically investigate the effect of the axial screw position in femoral neck fracture models fixed by three cannulated screws. Our hypothesis in this FEA study is that a more anterior screw position increases the bone-screw construct's resistance to posterior bending forces, thereby enhancing fixation stability.

Methods

Finite element model

In this study, we utilized a three-dimensional finite element model using a combination of medical imaging methods (computed tomography; CT), computer aided design and Mimics software [20–22]. The left femur underwent CT scanning at 1-mm intervals. The three-dimensional geometry of the femur and medullary canal surfaces was then accurately reconstructed from the CT images of a healthy male using Mimics software (version 23.0, Materialise, Leuven, Belgium). It was then stacked in three dimensions to obtain the line and surface of the entire femoral shape. Next, an intact femoral shape with a 125° neck-shaft angle was obtained from the geometric data. This shape was further processed for volume meshing using isotropic tetrahedral element types. To verify the developed finite element model, the strain was measured from a total of 20 points on the anterior, posterior, medial, and lateral sides of the model by attaching strain gauges, and the results were compared with data from previous studies [21]. The osteoporotic bone model was produced by following a previously validated method based on cortical thickness index [23]. Cortical thickness index serves as an important indicator that can define the shape of the femur and predict the degree of osteoporosis. According to Köse et al. [23], cortical thickness index can predict the degree of bone mineral density reduction based on the cortical thickness of the femur. This enables a more accurate reflection of the mechanical properties of the bone in osteoporotic conditions. As the cortical thickness index decreases, the density and strength of the cancellous bone also decrease, which weakens the structural integrity of the bone and significantly impacts its mechanical properties in osteoporotic patients. These changes were reflected in the finite element model by adjusting the material properties of the cancellous bone, allowing the effects of osteoporosis to be assessed. Pauwels type II femoral neck fractures with a 50° angle between the fracture line and femoral shaft axis were reproduced using the automatic solid and mesh generation program (ABAQUS) (version 6.14; Dassault Systems, Paris, France). To examine biomechanically significant changes in each model, the fracture gap was set to 2 mm.

In this study, 6.5-mm cannulated screws (Stryker, Mahwah, NJ, USA) were used. The geometries of all screw configurations were constructed within the femoral head of each model using ABAQUS. Three cannulated screws were inserted into the lateral cortex just above the lower margin of the lesser trochanter and parallel to the femoral neck axis at an angle of 125° from the femoral shaft in the AP view. Three cannulated screws were inserted in parallel into an inverted triangular pattern to ensure optimal stability [24–26]. All screws were positioned within 5 mm of the subchondral bone of the femoral head.

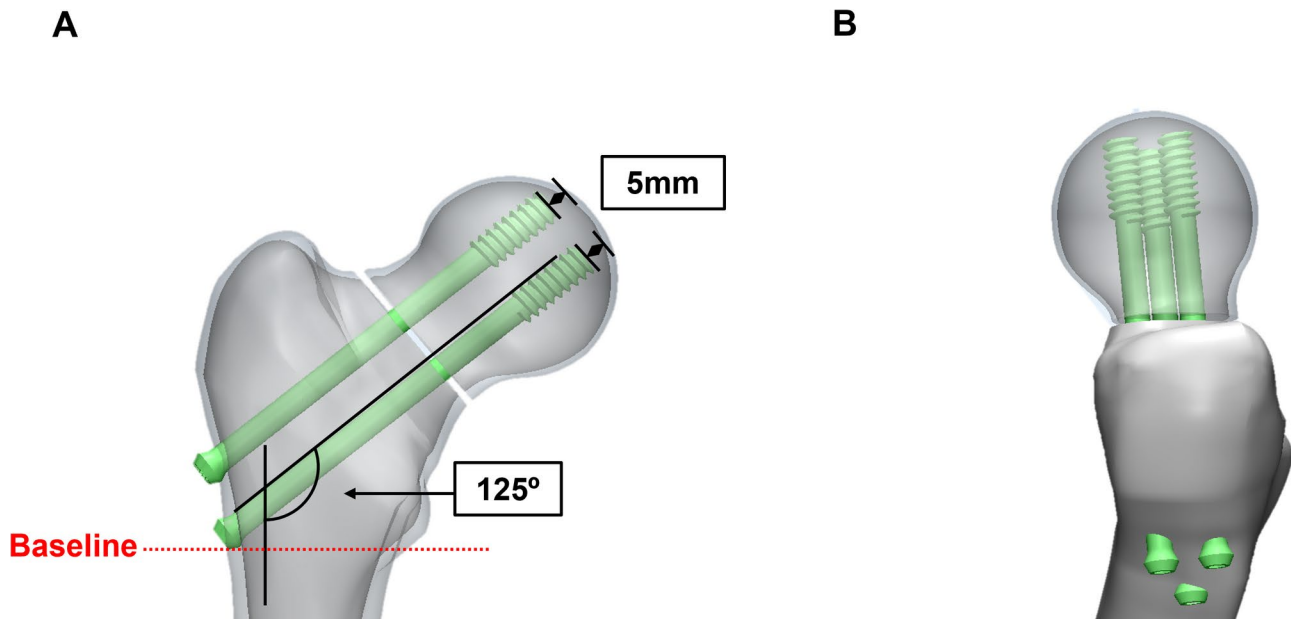


Fig. 1 Position of the cannulated screw in anteroposterior (a) and axial (b) view

Table 1 Material properties applied for the finite element model analysis

| | | Elastic Modulus(E) (MPa) | Poisson's ratio(ν) |
|-----------------|-------------------|-----------------------------|-----------------------------|
| Cortical bone | | 17,000 | 0.3 |
| Cancellous bone | Normal bone | 920 | 0.2 |
| | Osteoporotic bone | 574 | 0.2 |
| Screw (Ti6Al4V) | | 113,800 | 0.342 |

Anatomical reduction was assumed in all the models while maintaining the fracture gap (Fig. 1).

Material properties

The FEA assumes that the bone structure has homogeneous and isotropic linear properties. To create a femoral model with cancellous bone properties, the elastic modulus (E) was calculated based on an average CT Hounsfield unit value of 120.8 [27]. The relationship between Hounsfield unit and elastic modulus was analyzed [28, 29]:

$$\rho = 131,000 + 1067 \text{ HU}$$

$$E = 6850 \rho^{1.49}$$

where ρ is the apparent density (g/cm^3) and the unit of E is MPa. The material properties of the femoral cortical bone and screw were investigated based on earlier publications (Table 1) [30]. Based on young adult patients with an average age of less than sixty, material properties were assigned according to the cortical and cancellous regions [31, 32]. Additionally, osteoporotic properties were

considered to assess their impact on elderly patients with osteoporosis [33, 34]. For cancellous bone, we assumed the elastic modulus is proportional to the squared apparent density [35]. Typically, individuals experience an 8% loss of bone mass per decade starting at age 40, accompanied by a 66% reduction in elastic modulus [36]. Therefore, the elastic modulus of cancellous bone was reduced by 66% from the value used for the normal femoral bone [34]. For the purpose of the analysis, titanium alloy (Ti6Al4V) was used for the cannulated screws (Young's modulus, 113800 MPa; Poisson ratio, 0.3). Different material properties were assigned to different femoral regions.

Boundary and loading conditions

Assuming normal ambulation in the one-leg stance, hip joint reaction forces (2100 N, 300% of the body weight) were loaded onto the femoral head, and an abductor muscle force (700 N, 100% of the body weight) was applied to the lateral surface of the greater trochanter [37, 38]. Each force was applied at an angle of 20° from the vertical line in the frontal plane. The loading conditions are shown in Fig. 2 and specific magnitude of applied forces for loading conditions are shown in Table 2. A "tie" contact condition was applied in this study, assuming full constraints between bone-to-bone and bone-to-screw interfaces. A general contact condition was applied using a friction coefficient of 0.42 to allow optimal movement between the screw and bone [39].

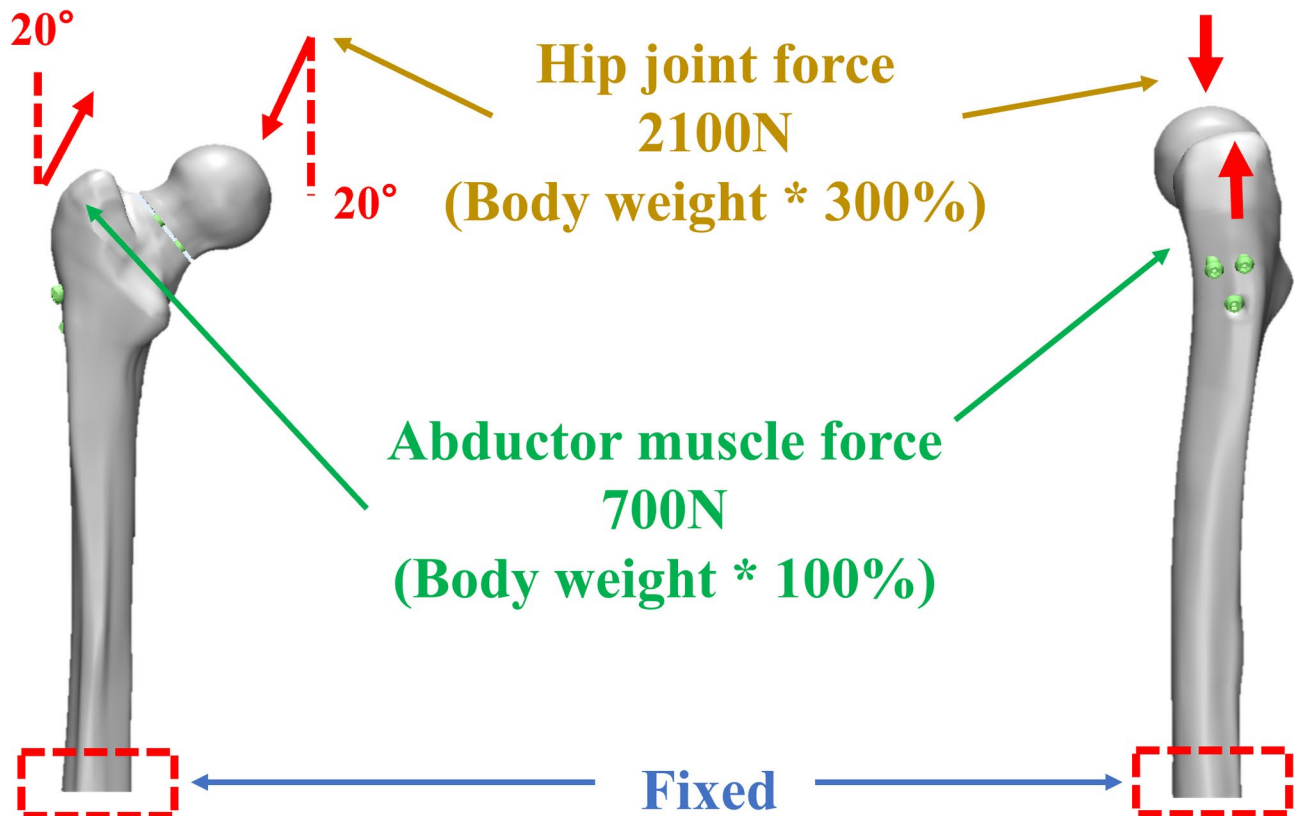


Fig. 2 Loading condition of the analysis model; Hip joint force, 2100 N (body weight X 300%); Abductor muscle force, 700 N (body weight X 100%)

Table 2 Magnitude of applied forces for normal walking loading conditions [1]

| | | $F_x(N)$ | $F_y(N)$ | $F_z(N)$ |
|----------------|----------------------------|----------|----------|----------|
| Normal walking | Hip contact reaction force | -432 | -1833.6 | -262.4 |
| | Abductor muscles | 464 | 692 | 34.4 |

1. Taylor M: Finite element analysis of the resurfaced femoral head. *Proc Inst Mech Eng H* 2006, 220(2):289–297

Finite element model analysis

Nine models were analyzed using combinations of three different screw positions (anterior, central, and posterior) in the axial view and three different models (type 1: 8° angles, 10 mm inter-screw interval; type 2: 6° angles, 10 mm inter-screw interval; type 3: 8° angles, 6 mm inter-screw interval) in normal and osteoporotic bone models (Fig. 3).

Stability refers to the reduction of stress concentration at the bone-screw construct and the minimization of micromotion, both of which are critical factors for enhancing fixation longevity and osseointegration [40, 41]. Therefore, we investigate stress concentration on the screws and bone as well as interfragmentary displacement. The peak von Mises stresses (PVMSs) and mean stress over a region of interest (ROI) were measured in each model and compared with the yield strength of the cannulated screw and bone. The regions exhibiting PVMSs on the screw and femoral bone were designated

as ROIs for each model. To investigate the stress concentration around the cannulated screw, the PVMS and mean stress were measured at the screw and lateral cortex of the femoral bone around the screw and around the screw tip within the femoral head for each model. The obtained measurements were then compared with the yield strength of the screw and femoral bone. The yield strength of the screw-bone construct was obtained from previous studies (Ti6Al4V, 880 MPa; cortical bone, 118 MPa; and cancellous bone, 22 MPa) [42]. Moreover, each interfragmentary displacement component (axial, anterior-posterior shear, or superior-inferior shear) was measured to evaluate the interfragmentary stability (Fig. 4).

Results

Stress distribution at the cannulated screws

Stress concentration on the cannulated screws was observed at the inferior screw around the fracture site in all models, regardless of the screw position. Therefore, the inferior screw around the fracture site was designated as the ROI for the cannulated screws in each model. In the axial view, all PVMSs on the screw increased as the screw position moved from anterior to posterior within the femoral head. Meanwhile, these PVMSs decreased as the tilting angle of the screws increased or

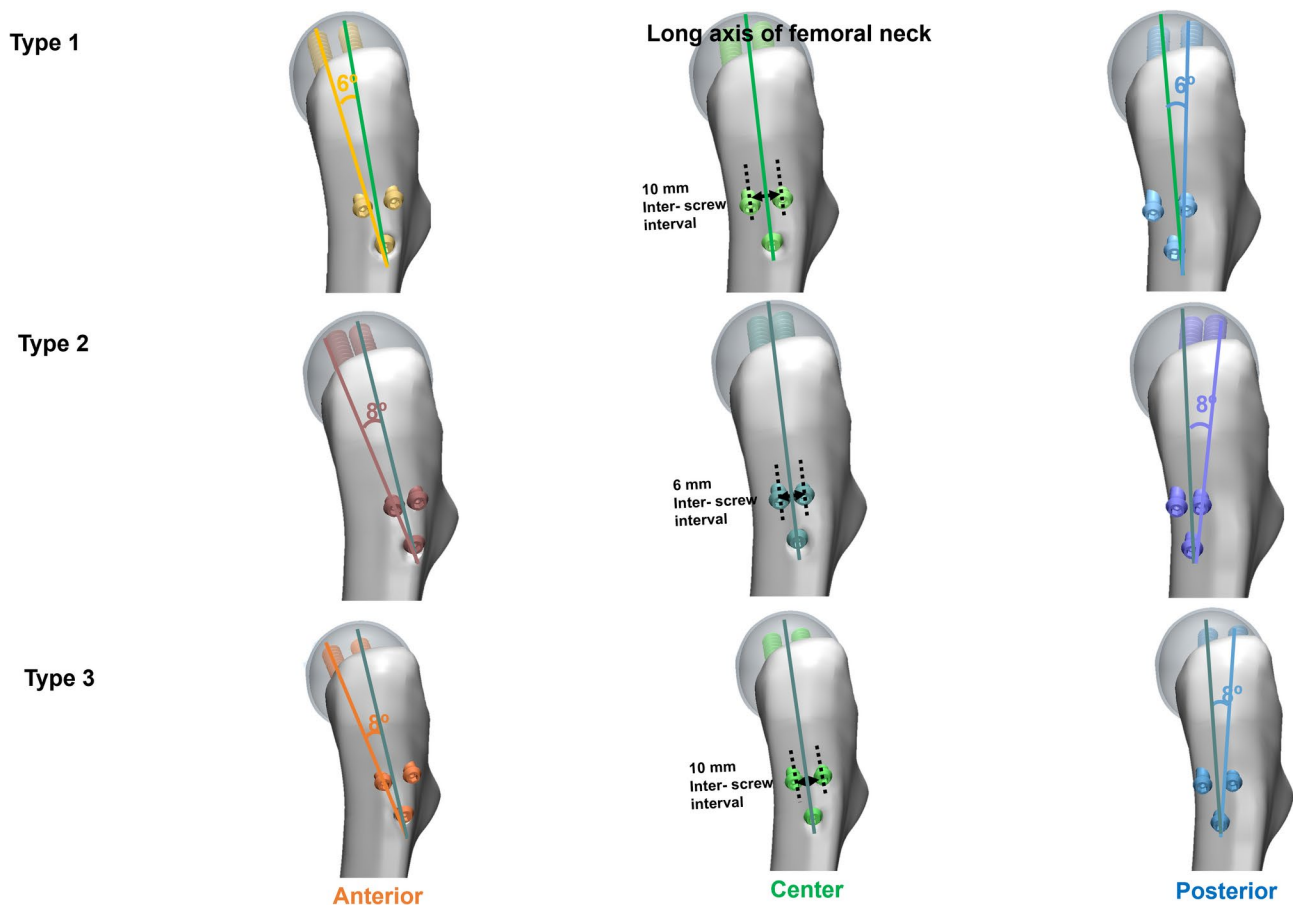


Fig. 3 The figure of nine group models. (type 1: 8° angles, 10 mm inter-screw interval; type 2: 6° angles, 10 mm inter-screw interval; type 3: 8° angles, 6 mm inter-screw interval)

the inter-screw interval widened as much as possible. All PVMSs in each type 3 finite element model were greater than those observed in type 2. The mean stresses on the screw in all models showed patterns similar to those of the PVMSs (Fig. 5).

In osteoporotic bone models, the stress concentration on the cannulated screw showed a pattern similar to that observed in normal bone models. However, all figures in each model were greater than those observed in the normal bone models. Consequently, the PVMS was highest in the finite element model with a 6 mm inter-screw interval and a cannulated screw positioned 8° posteriorly (type 3) in the osteoporotic bone models. The PVMS of the finite element model in type 3 was close to the yield strength (841 MPa, 95.6% of the yield strength) (Supplementary Fig. 1). All the mean stresses of the screw in each model were lower than the yield strength of the screw (Ti6Al4V, 880 MPa). Table 3 presents the mean stresses and increase rates of all models compared with type 1, which had an anteriorly positioned screw in the normal bone model.

Stress distribution on the femoral bone

Stress concentration on the femoral bone was observed around the inferior screw hole in the lateral cortex and around the inferior screw tip within the femoral head in all models. Therefore, we designated these two points as the ROIs for the femoral bone in each model. The stress concentration on the femoral bone around the screw exhibited a pattern similar to that observed in the cannulated screw. All PVMSs on the bone around the screw tended to increase as the screw position moved from anterior to posterior in the axial view. Meanwhile, these PVMSs decreased as the tilting angle of the screws increased or the inter-screw interval widened as much as possible.

The mean stresses in all models showed similar patterns to those of the PVMSs. All mean stresses in the models of cortical and cancellous bones were lower than the yield strength of the femoral bone (cortical bone, 118 MPa; cancellous bone, 22 MPa). However, all PVMSs at the lateral cortex in all models with posteriorly positioned screws were either comparable to or greater than the yield strength. Furthermore, in osteoporotic models, all PVMSs at the lateral cortex were greater than the yield

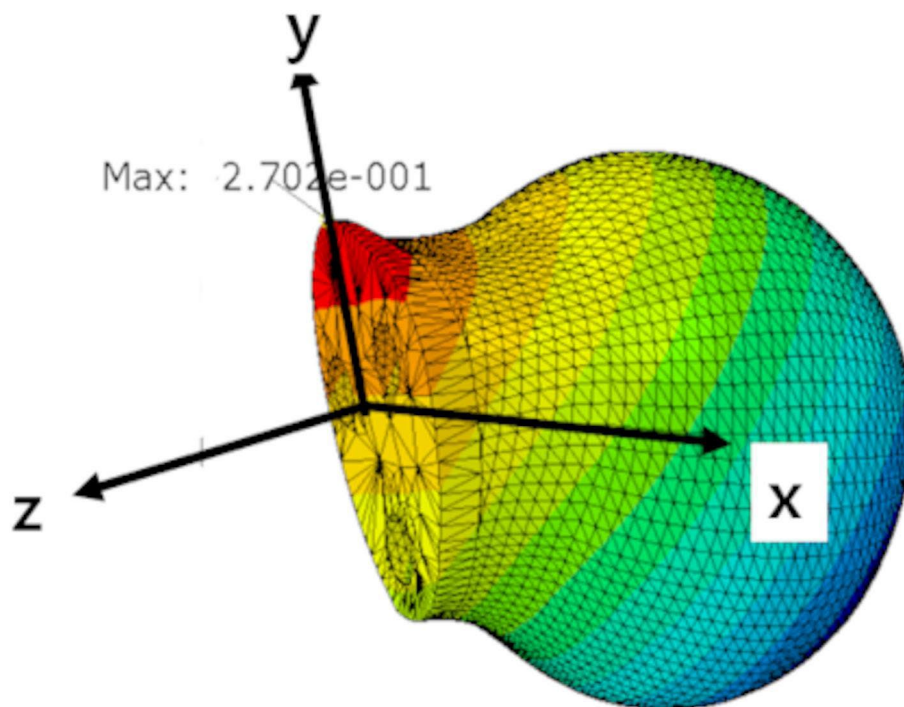


Fig. 4 Local coordinate system considered at fracture plane which shows the direction of shear and axial displacements

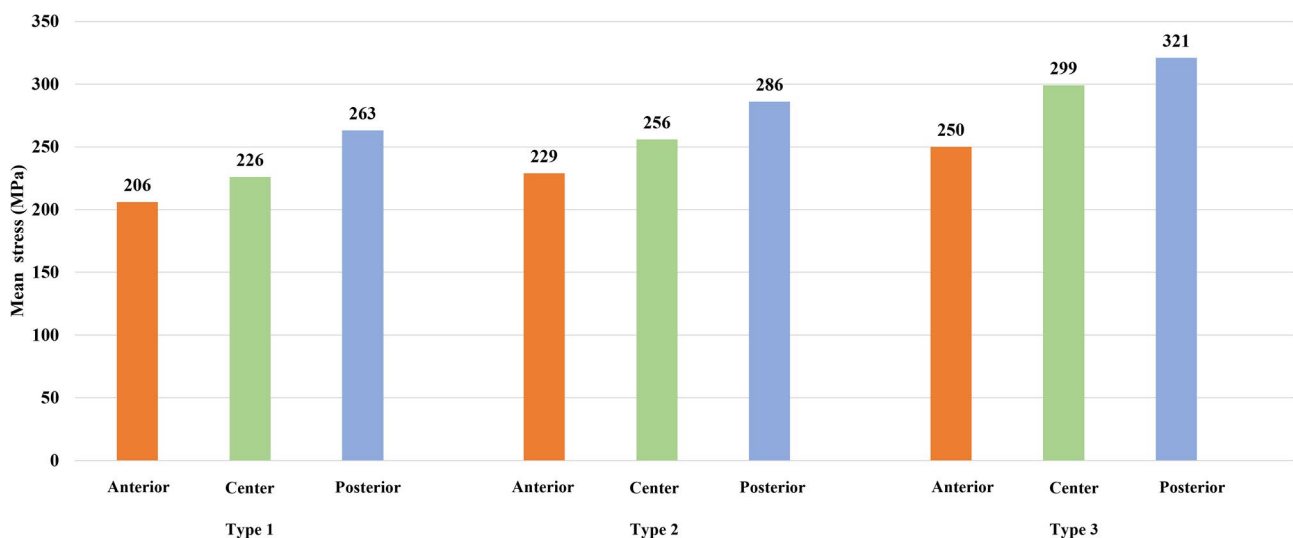


Fig. 5 Result of the mean stress over a region of interest on the screw in each finite element model

strength, except for the PVMS in the type 1 finite element model with an anteriorly positioned screw. Detailed figures of the PVMS for all models are provided in Table 4.

Interfragmentary displacement at the fracture site

The maximal values of the interfragmentary displacement component (axial, anterior-posterior shear, or superior-inferior shear) showed no significant difference or pattern. The values of the displacement for each direction were consistently similar in all models. Although the

absolute displacement values slightly differed between each direction, all values showed below 5-mm displacement in each direction regardless of the finite element model and screw positions. Detailed figures of the interfragmentary displacement for all models are provided in supplementary Table 1.

Table 3 Results of mean stress over a region of interest of the cannulated screw in finite element models

| | | | Mean stress (MPa) | Increase rate (%) |
|-------------------|--------|-----------|-------------------|-------------------|
| Normal bone | Type 1 | Anterior | 206 | |
| | | Center | 226 | 9.7 |
| | | Posterior | 263 | 27.7 |
| | Type 2 | Anterior | 229 | 11.2 |
| | | Center | 256 | 24.3 |
| | | Posterior | 286 | 38.8 |
| | Type 3 | Anterior | 250 | 21.4 |
| | | Center | 299 | 45.1 |
| | | Posterior | 321 | 55.8 |
| Osteoporotic bone | Type 1 | Anterior | 223 | 8.3 |
| | | Center | 257 | 24.8 |
| | | Posterior | 291 | 41.3 |
| | Type 2 | Anterior | 254 | 23.3 |
| | | Center | 280 | 35.9 |
| | | Posterior | 307 | 49.0 |
| | Type 3 | Anterior | 290 | 40.8 |
| | | Center | 325 | 57.8 |
| | | Posterior | 385 | 86.9 |

The increase rate of mean stress over a region of interest compared to type 1 with an anteriorly positioned screw in normal bone model

Type 1: 8° angles, 10 mm inter-screw distance, Type 2: 6° angles, 10 mm inter-screw distance; Type 3: 8° angles, 6 mm inter-screw distance

Table 4 Results of peak von mises stress of the lateral cortex and femoral head in finite element models (MPa)

| | | | Cortical bone [‡] | Cancellous bone [†] |
|-------------------|--------|-----------|----------------------------|------------------------------|
| Normal bone | Type 1 | Anterior | 102 | 10.4 |
| | | Center | 113 | 11.8 |
| | | Posterior | 117 | 12.4 |
| | Type 2 | Anterior | 110 | 11.7 |
| | | Center | 115 | 13.3 |
| | | Posterior | 127* | 15.7 |
| | Type 3 | Anterior | 117 | 12.8 |
| | | Center | 122* | 14.6 |
| | | Posterior | 123* | 16.6 |
| Osteoporotic bone | Type 1 | Anterior | 110 | 12.9 |
| | | Center | 121* | 14.0 |
| | | Posterior | 130* | 16.9 |
| | Type 2 | Anterior | 118* | 13.3 |
| | | Center | 124* | 16.0 |
| | | Posterior | 136* | 18.5 |
| | Type 3 | Anterior | 127* | 13.5 |
| | | Center | 139* | 17.3 |
| | | Posterior | 170* | 22.5* |

* Higher than the yield strength (MPa): cortical bone 118; cancellous bone 22

Type 1: 8° angles, 10 mm inter-screw distance, Type 2: 6° angles, 10 mm inter-screw distance; Type 3: 8° angles, 6 mm inter-screw distance

‡: Measured at the lateral cortex around the inferior screw head

†: Measured at the inferior screw tip within the femoral head

Discussion

This FEA study was conducted to investigate the stress concentration at the screw-bone construct and subsequent fixation stability according to the axial screw position in femoral neck fracture models fixed with three cannulated screws. The present study showed that the anterior screw position in the axial plane reduces stress concentration and enhances fixation stability of the screw-bone construct after three cannulated screws fixation under the assumption that the inter-screw interval is as wide as possible in femoral neck fractures.

As well known, three cannulated screws should be inserted as wide as possible to enhance the fixation stability for these fractures [10, 13]. Some studies suggest inserting the additional fourth screw in a diamond configuration or augmenting the fixation system with a buttress plate [6, 43]. Despite these efforts, a definitive conclusion has not yet been reached. Although numerous studies have attempted to change the fixation direction and employ new devices in the coronal plane, there is a notable lack of research focusing on the axial plane. Recently, biomechanical and clinical studies demonstrated the posterior, fully threaded positioning screw increases fixation stability in the axial plane for femoral neck fractures fixed with three cannulated screws [15, 17]. However, the existing literature lacks evidence on the enhanced fixation stability associated with the axial position of the cannulated screw. Therefore, we conducted this FEA study to evaluate the optimal axial position of screws to obtain more stable fixation in cannulated screw fixation for femoral neck fractures.

In the current study, the PVMS and mean stress on the screw-bone construct increased as the axial screw position moved from anterior to posterior, and the inter-screw interval was narrow in femoral neck fracture models fixed with three cannulated screws. Our results align with the well-known principle that a greater spread of screws leads to increased stability [10, 13]. Additionally, the stress concentration increased as the screw position moved from anterior to posterior in the axial view in this study. We believe that the fixation with the anterior screw position was more resistant to posterior bending forces under axial loading compared to the different screw positions, leading to great resistance to the dorsal slipping of the femoral head.

Posterior tilt of the femoral head is often a concern due to trauma mechanism and hip anatomy [44]. The femoral neck exhibits an anatomical characteristic of anteversion ranging from 10° to 15°. Consequently, when axial loading occurs during walking, the femoral neck is subjected to a posterior bending force [45–47]. For this reason, valgus impaction and posterior tilt were frequently observed in femoral neck fractures. The risk of fixation failure may remain due to postoperative posterior tilt

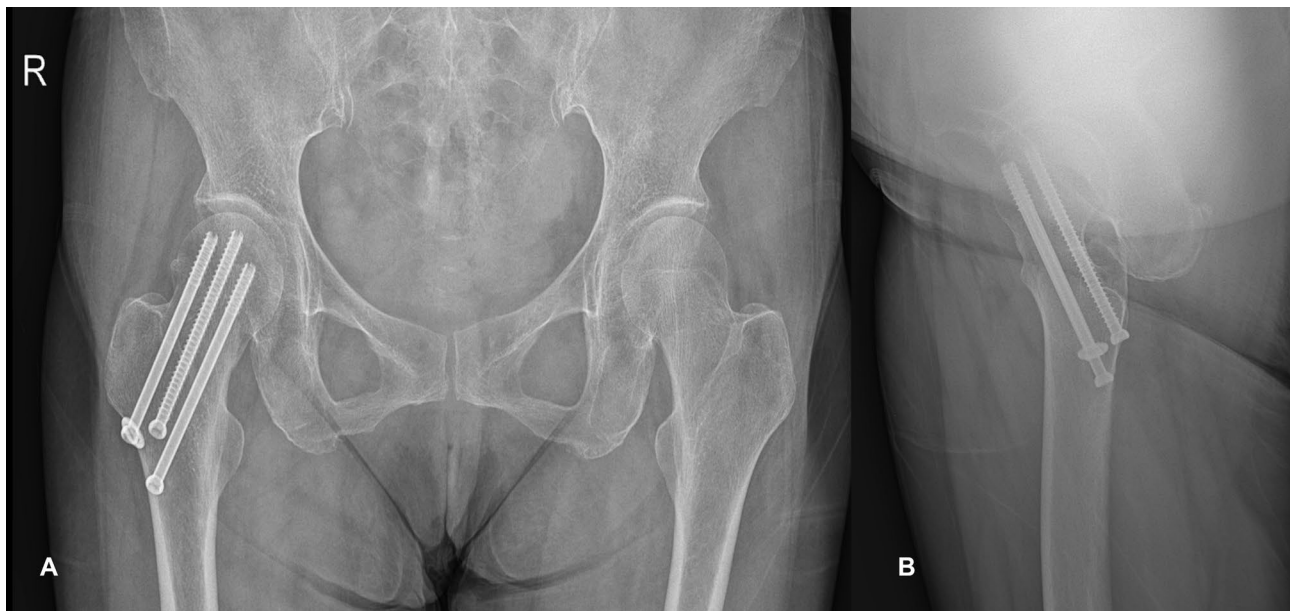


Fig. 6 64-year-old female patient fixed with three cannulated screws for femoral neck fracture in anteroposterior (a) and axial (b) view

because this bending force continues even after fixation with three cannulated screws. A previous biomechanical study showed that the proximal fragment tilts posteriorly, called retroversion, after applying the axial loading [48]. Therefore, we propose inserting the screws as anteriorly as possible to be more resistant to posterior bending force in cannulated screw fixation for femoral neck fractures (Fig. 6). However, cannulated screw fixation for femoral neck fracture in elderly patients should be performed with more caution under limited conditions, considering our findings that more stress concentration was observed at osteoporotic bone in types 2 and 3.

However, determining a numerically tolerable range for the anterior position of the screws is difficult because the maximum tilt angle of screws, considering their safety, can be changeable according to each patient's femoral geometry and size. Too eccentric screw insertion within the femoral head makes the screw length excessively short, leading to uneven stress distribution, and may subsequently increase the risk of fixation failure. In the finite element model simulated in this study, the 8-degree tilt of screw position within the femoral head was the maximum angle maintaining the screw length as long as possible compared to when inserting the screw into the center of the femoral head. Hence, based on our results, we believe that cannulated screws should not be inserted posteriorly and should be placed slightly anteriorly within about 8 degrees in this model. We set an inter-screw interval of 10 mm as wide as possible to increase fixation stability depending on the size and geometry of this model. Consequently, we reproduced an inter-screw interval of 10 mm and a tilt angle of 8 degrees at maximum. When we set the tilt angle within 5 degrees, there

were no differences among finite element model. Besides, when we set the inter-screw interval less than 6 mm, the screw head overlap occurred at the lateral cortex. Accordingly, a 6-degree tilt model (type 2) and a 6-mm interval model (type 3) were reproduced as comparison groups to investigate the difference in stress concentration according to the changes in the inter-screw interval and tilt angle. When comparing the increase rates of stress concentration at identical screw positions, the increase rate between type 1 and 3 was much higher than between type 1 and 2. We believe that the inter-screw interval is a more important factor than the screw tilt angle for a more stable screw-bone construct. Therefore, we should strive to insert the cannulated screws as anteriorly as possible while keeping the inter-screw interval as wide as possible for a more stable screw-bone construct in femoral neck fractures.

Interfragmentary movement can influence the process of fracture healing and serve as a crucial indicator for assessing fixation stability [49]. Samsami et al. [50] reported that cannulated screw fixation showed higher interfragmentary movement and least stable fixation than dynamic hip screw with derotational screw in vertical femoral neck fractures. Consequently, cannulated screw fixation is unable to provide appropriate fixation for bone healing. On the contrary, in this study, the interfragmentary displacement of the finite element model in each direction did not show a difference or pattern. And all values measured in this experiment were very small, less than 5 mm, regardless of the model and screw positions. In other words, this can be seen as meaning that all the models we represented with Pauwels type II femoral

neck fractures with cannulated fixation had adequate fixation stability for fracture healing.

This study has some limitations. First, the complex physiological force components around the proximal femur during normal ambulation were simplified, though physiologic loading is more complex, and real-life situations can involve greater loading. However, only axial loading used to simulate the forces of a one-legged stance was considered appropriate for this FEA because protected weight-bearing with walking aids after surgery is advised until bony union is achieved. Second, instead of modeling the actual screw insertion process, 'Boolean operations' were used to simplify the screw insertion state. Boolean operations define the geometric relationship between the screw and the insertion site representing the inserted state of the screw without considering physical interactions or pressure distribution. While this approach increases computational efficiency and simplifies complex physical processes, it does not account for fine physical deformations, frictional forces, displacement between screw and bone, or pressure distributions resulting from screw insertion. As a result, there may be limitations in predicting pull-out strength of screws [51]. Third, this study was conducted solely under linear static conditions. Therefore, we focused on the risk of fixation failure or refracture during the early postoperative period until bony union was achieved and could not consider fatigue fracture requiring long-term cyclic loading. Fourth, the friction coefficient used in this study may not be consistent across all implants, as it can vary depending on the type of implant, surface treatment, and coating technology. In particular, advancements in coating technologies can alter the friction coefficient, which should be considered an important limitation [52]. Such technological advancements can influence the stability of implants, and future studies should account for the variability of the friction coefficient by incorporating different surface treatments and coating technologies into the modeling process. Fifth, the exact interactions between the screw and bone, as well as the proximal and distal fragments, could be not determined. Although friction coefficients in the current study were applied under the assumption of general contact conditions at the contact interfaces, it was difficult to accept these values for perfect reproducibility, as it was challenging to determine the precise interactions at each interface. Finally, it is yet difficult to clinically validate our results, as this is an experimental study using FEA. We conducted this experimental study using a simplified finite element model. Of course, femoral neck fractures have various types. However, the aim of this study is to discuss the differences based on screw position by simplifying the fracture line to a single type. Moreover, we do not consider the values in this study to be numerically precise or definitive.

Nevertheless, we believe that this study indicates that anterior screw position on the axial plane is more appropriate to reduce stress concentration at the screw-bone construct and enhance the fixation stability during three cannulated screw fixations in femoral neck fractures.

Despite the aforementioned limitations, to the best of our knowledge, this is the first FEA to investigate stress concentration at the screw-bone construct according to different screw positions in the axial plane within the femoral head in femoral neck fractures fixed with three cannulated screws in young patients as well as the elderly with osteoporosis and to suggest more appropriate axial screw positions in these fractures. However, further large multi-center clinical studies are required to substantiate our results and verify the importance of the anterior position of cannulated screws in the axial plane.

Conclusions

Our FEA study revealed that the stress concentration on the screw-bone constructs increases as the screw position within the femoral head moves from anterior to posterior in the axial view in femoral neck fracture models fixed with three cannulated screws. Considering the stress concentrations at the screws and the femoral bone around the screws in femoral neck fracture models fixed with three cannulated screws, the screws should be positioned anterior to the center on the axial view, and the inter-screw interval should be maximized as much as possible depending on the patient's femur geometry to increase the fixation stability of the screw-bone construct when femoral neck fractures are treated with three cannulated screws.

Abbreviations

| | |
|------|-------------------------|
| AP | Anteroposterior |
| FEA | Finite element analysis |
| CT | Computed tomography |
| PVMS | Peak von Mises stresses |
| ROI | Region of interest |

Supplementary Information

The online version contains supplementary material available at <https://doi.org/10.1186/s12891-025-08681-1>.

Supple Fig. 1. Result of the peak von Mises stress on the screw in each finite element model (osteoporosis)

Supplementary Material 2

Author contributions

DK Kwak designed the study and wrote the manuscript. YJ Lee investigated and analyzed data. SJ Lee collected data and validated the methodology. SH Lee analyzed the data. The design of the study and interpretation of data was done jointly by all authors. JH Yoo designed and supervised the study, and revised the final draft critically for important intellectual content and approved the version to be submitted the manuscript.

Funding

This study was supported by the Hallym University Research Fund 2024 (HURF-2024-03).

Data availability

The datasets used and/or analyzed in this study are available from the corresponding author on reasonable request.

Declarations

Ethics approval and consent to participate

Not applicable. It did not report on or involve the use of any animal or human data or tissue in this study. It was an experimental study.

Consent for publication

Not applicable.

Competing interests

The authors declare no competing interests.

Received: 22 July 2024 / Accepted: 18 April 2025

Published online: 30 April 2025

References

1. Yeo I, Lim S-J. Current treatment strategy for young adult femur neck fractures. *J Korean Orthop Association* 2015, 50(3).
2. Ly TV, Swiontkowski MF. Treatment of femoral neck fractures in young adults. *J Bone Joint Surg Am*. 2008;90(10):2254–66.
3. Liang C, Yang F, Lin W, Fan Y. Efficacies of surgical treatments based on Harris hip score in elderly patients with femoral neck fracture. *Int J Clin Exp Med*. 2015;8(5):6784–93.
4. Cordero-Ampuero J, Descalzo I, Fernández-Villacañas P, Berdullas JM, Hernández-Rodríguez A, de Quadros J, Marcos-Aguilar S, Peix C. Retrospective paired cohort study comparing internal fixation for undisplaced versus hemiarthroplasty for displaced femoral neck fracture in the elderly. *Injury*. 2024;55(Suppl 5):111674.
5. Cui S, Wang D, Wang X, Li Z, Guo W. The choice of screw internal fixation and hemiarthroplasty in the treatment of femoral neck fractures in the elderly: a meta-analysis. *J Orthop Surg Res*. 2020;15(1):433.
6. Jiang D, Zhan S, Wang L, Shi LL, Ling M, Hu H, Jia W. Biomechanical comparison of five cannulated screw fixation strategies for young vertical femoral neck fractures. *J Orthop Res*. 2021;39(8):1669–80.
7. Jung CH, Cha Y, Yoon HS, Park CH, Yoo JI, Kim JT, Jeon Y. Mechanical effects of surgical variations in the femoral neck system on Pauwels type III femoral neck fracture: a finite element analysis. *Bone Joint Res*. 2022;11(2):102–11.
8. Jiang D, Zhan S, Cai Q, Hu H, Jia W. Long-term differences in clinical prognosis between crossed- and parallel-cannulated screw fixation in vertical femoral neck fractures of non-geriatric patients. *Injury*. 2021;52(11):3408–14.
9. Rajnish RK, Srivastava A, Rathod PM, Haq RU, Aggarwal S, Kumar P, Dhammi IK, Dadra A. Does the femoral neck system provide better outcomes compared to cannulated screws fixation for the management of femoral neck fracture in young adults? A systematic review of literature and meta-analysis. *J Orthop*. 2022;32:52–9.
10. Zdero R, Keast-Butler O, Schemitsch EH. A Biomechanical comparison of two triple-screw methods for femoral neck fracture fixation in a synthetic bone model. *J Trauma*. 2010;69(6):1537–44.
11. Stockton DJ, Lefavre KA, Deakin DE, Osterhoff G, Yamada A, Broekhuysen HM, O'Brien PJ, Slobogean GP. Incidence, magnitude, and predictors of shortening in young femoral neck fractures. *J Orthop Trauma*. 2015;29(9):e293–298.
12. Erivan R, Fassot G, Villatte G, Mulliez A, Descamps S, Boisgard S. Results of femoral neck screw fixation in 112 under 65-years-old at a minimum 2 years' follow-up. *Orthop Traumatology: Surg Res*. 2020;106(7):1425–31.
13. Gurusamy K, Parker MJ, Rowlands TK. The complications of displaced intracapsular fractures of the hip: the effect of screw positioning and angulation on fracture healing. *J Bone Joint Surg Br*. 2005;87(5):632–4.
14. Conn KS, Parker MJ. Undisplaced intracapsular hip fractures: results of internal fixation in 375 patients. *Clin Orthop Relat Res* 2004(421):249–54.
15. Shin KH, Hong SH, Han SB. Posterior fully threaded positioning screw prevents femoral neck collapse in garden I or II femoral neck fractures. *Injury*. 2020;51(4):1031–7.
16. Zhang B, Liu J, Zhu Y, Zhang W. A new configuration of cannulated screw fixation in the treatment of vertical femoral neck fractures. *Int Orthop*. 2018;42(8):1949–55.
17. Schaefer TK, Spross C, Stoffel KK, Yates PJ. Biomechanical properties of a posterior fully threaded positioning screw for cannulated screw fixation of displaced neck of femur fractures. *Injury*. 2015;46(11):2130–3.
18. Jiang X, Liang K, Du G, Chen Y, Tang Y, Geng K. Biomechanical evaluation of different internal fixation methods based on finite element analysis for Pauwels type III femoral neck fracture. *Injury* 2022.
19. Wang M, Wang Y, Zou F, Tan L, Wang Y. Mechanical study of the application of compression screw nails in the cross-inverted triangular pattern for internal fixation of femoral neck fractures. *BMC Musculoskelet Disord*. 2023;24(1):350.
20. Kwon GJJM, Oh JK, Lee SJ. Effects of screw configuration on Biomechanical stability during extra-articular complex fracture fixation of the distal femur treated with locking compression plate. 2010.
21. Heiner AD, Brown TD. Structural properties of a new design of composite replicate femurs and tibias. *J Biomech*. 2001;34(6):773–81.
22. Cristofolini L, Viceconti M, Cappello A, Toni A. Mechanical validation of whole bone composite femur models. *J Biomech*. 1996;29(4):525–35.
23. Köse Ö, Kılıçaslan ÖF, Arık HO, Sarp Ü, Toslak İE, Uçar M, Başaran S, Evlice A, Erdem M, Demirkıran M. Prediction of osteoporosis through radiographic assessment of proximal femoral morphology and texture in elderly; is it valid and reliable? *Türk Osteoporoz Dergisi*. 2015;21(2):46–52.
24. Szita J, Cserhádi P, Bosch U, Manninger J, Bodzay T, Fekete K. Intracapsular femoral neck fractures: the importance of early reduction and stable osteosynthesis. *Injury*. 2002;33(Suppl 3):C41–46.
25. Bonnaire FA, Weber AT. Analysis of fracture gap changes, dynamic and static stability of different osteosynthetic procedures in the femoral neck. *Injury*. 2002;33(Suppl 3):C24–32.
26. Oakey JW, Stover MD, Summers HD, Sartori M, Havey RM, Patwardhan AG. Does screw configuration affect subtrochanteric fracture after femoral neck fixation? *Clin Orthop Relat Res*. 2006;443:302–6.
27. Lee S, Chung CK, Oh SH, Park SB. Correlation between bone mineral density measured by Dual-Energy X-Ray absorptiometry and Hounsfield units measured by diagnostic CT in lumbar spine. *J Korean Neurosurg Soc*. 2013;54(5):384–9.
28. Rho JY, Hobatho MC, Ashman RB. Relations of mechanical properties to density and CT numbers in human bone. *Med Eng Phys*. 1995;17(5):347–55.
29. Morgan EF, Bayraktar HH, Keaveny TM. Trabecular bone modulus-density relationships depend on anatomic site. *J Biomech*. 2003;36(7):897–904.
30. Stoffel K, Dieter U, Stachowiak G, Gächter A, Kuster MS. Biomechanical testing of the LCP—how can stability in locked internal fixators be controlled? *Injury*. 2003;34(Suppl 2):B11–19.
31. Evans FG. Mechanical properties and histology of cortical bone from younger and older men. *Anat Rec*. 1976;185(1):1–11.
32. Turner CH, Rho J, Takano Y, Tsui TY, Pharr GM. The elastic properties of trabecular and cortical bone tissues are similar: results from two microscopic measurement techniques. *J Biomech*. 1999;32(4):437–41.
33. Gardner TN, Stoll T, Marks L, Mishra S, Knothe Tate M. The influence of mechanical stimulus on the pattern of tissue differentiation in a long bone fracture—an FEM study. *J Biomech*. 2000;33(4):415–25.
34. Lotz JC, Cheal EJ, Hayes WC. Stress distributions within the proximal femur during gait and falls: implications for osteoporotic fracture. *Osteoporos Int*. 1995;5(4):252–61.
35. Rice JC, Cowin SC, Bowman JA. On the dependence of the elasticity and strength of cancellous bone on apparent density. *J Biomech*. 1988;21(2):155–68.
36. Mazess RB. On aging bone loss. *Clin Orthop Relat Res*. 1982;165:239–52.
37. Taylor M. Finite element analysis of the resurfaced femoral head. *Proc Inst Mech Eng H*. 2006;220(2):289–97.
38. Law GW, Wong YR, Yew AK, Choh ACT, Koh JSB, Howe TS. Medial migration in cephalomedullary nail fixation of Peritrochanteric hip fractures: A Biomechanical analysis using a novel bidirectional cyclic loading model. *Bone Joint Res*. 2019;8(7):313–22.
39. Lee PY, Lin KJ, Wei HW, Hu JJ, Chen WC, Tsai CL, Lin KP. Biomechanical effect of different femoral neck blade position on the fixation of intertrochanteric fracture: a finite element analysis. *Biomed Tech (Berl)*. 2016;61(3):331–6.

40. Gross S, Abel EW. A finite element analysis of Hollow stemmed hip prostheses as a means of reducing stress shielding of the femur. *J Biomech*. 2001;34(8):995–1003.
41. Baleani M, Cristofolini L, Viceconti M. Endurance testing of hip prostheses: a comparison between the load fixed in ISO 7206 standard and the physiological loads. *Clin Biomech (Bristol)*. 1999;14(5):339–45.
42. Bayraktar HH, Morgan EF, Niebur GL, Morris GE, Wong EK, Keaveny TM. Comparison of the elastic and yield properties of human femoral trabecular and cortical bone tissue. *J Biomech*. 2004;37(1):27–35.
43. Su Z, Liang L, Hao Y. Medial femoral plate with cannulated screw for Pauwels type III femoral neck fracture: A meta-analysis. *J Back Musculoskeletal Rehabil*. 2021;34(2):169–77.
44. Kalsbeek JH, van Walsum ADP, Roerdink WH, van Vugt AB, van de Krol H, Schipper IB. Validation of two methods to measure posterior Tilt in femoral neck fractures. *Injury*. 2020;51(2):380–3.
45. Tönnis D, Heinecke A. Acetabular and femoral anteversion: relationship with osteoarthritis of the hip. *J Bone Joint Surg Am*. 1999;81(12):1747–70.
46. Wilkinson JA. Femoral anteversion in the rabbit. *J Bone Joint Surg Br*. 1962;44-b:386–97.
47. Salter RB. Role of innominate osteotomy in the treatment of congenital dislocation and subluxation of the hip in the older child. *J Bone Joint Surg Am*. 1966;48(7):1413–39.
48. Kwak DK, Kim WH, Lee SJ, Rhyu SH, Jang CY, Yoo JH. Biomechanical comparison of three different intramedullary nails for fixation of unstable basicervical intertrochanteric fractures of the proximal femur: experimental studies. *Biomed Res Int*. 2018;2018:7618079.
49. von Rüden C, Augat P. Failure of fracture fixation in osteoporotic bone. *Injury*. 2016;47(Suppl 2):S3–10.
50. Samsami S, Augat P, Rouhi G. Stability of femoral neck fracture fixation: A finite element analysis. *Proc Inst Mech Eng H*. 2019;233(9):892–900.
51. Addeviso F, Solitro GF, Morandi MM. Salvaging Pull-Out strength in a previously stripped screw site: A comparison of three rescue techniques. *J Funct Morphol Kinesiol* 2021, 6(3).
52. Patel S, Solitro GF, Sukotjo C, Takoudis C, Mathew MT, Amirouche F, Shokuhfar T. Nanotopography and surface stress analysis of Ti6Al4V bioimplant: an alternative design for stability. *JOM*. 2015;67(11):2518–33.

Publisher's note

Springer Nature remains neutral with regard to jurisdictional claims in published maps and institutional affiliations.